Frontiers in Nanoscience and Nanotechnology

oat open access text

Research Article ISSN: 2397-6527

Compositional Tuning, Properties and Conversion of $In_{2x}Ga_{2-2x}O_3$ Nanowires Into I–III–VI$_2$ Chalcopyrite Cu (InxGa$_{1-X}$)S_2

Matthew Zervos[1]* and Andreas Othonos[2]

[1]Nanostructured Materials and Devices Laboratory, Department of Mechanical and Manufacturing Engineering, University of Cyprus, 20537, Nicosia, 1678, Cyprus

[2]Laboratory of Ultrafast Science, Department of Physics, University of Cyprus, 20537, Nicosia, 1678, Cyprus

Abstract

$In_{2x}Ga_{2-2x}O_3$ nanowires were grown at 800°C *via* the vapor-liquid-solid mechanism on Si(001) using 1 nm Au as a catalyst and by varying systematically the In to Ga ratio. The $In_{2x}Ga_{2-2x}O_3$ nanowires have average diameters of ≈ 50 nm, lengths up to 100 μm and consist of a mixture of phases belonging to the cubic bixbyite In_2O_3 and monoclinic β-Ga_2O_3. The nanowires exhibited room temperature photoluminescence at 3.1 eV which shifted to the blue upon increasing the content of Ga. In contrast we observe a strong red-shift from 3.1 eV to 1.8 eV after processing under H_2S at 700°C due to the diffusion of S into oxygen vacancies and the formation of Ga rich $In_{2x}Ga_{2-2x}S_3$. We find that the deposition of Cu over $In_{2x}Ga_{2-2x}O_3$ and conversion under H_2S between 100°C to 500°C resulted into the formation of $Cu(In_xGa_{1-x})S_3$ nanowires with smaller resistances and a stronger red shift in the photoluminescence from 3.1 eV to 1.5 eV close to the energy gap of $Cu(In_xGa_{1-x})S_2$.

Introduction

Metal oxide (MO) semiconductor nanowires (NWs) such as ZnO [1], SnO_2 [2], In_2O_3 [3], Sn doped In_2O_3 [4] and Ga_2O_3 [5] have been investigated and used extensively for the fabrication of nanoscale devices such as sensors, solar cells, photo detectors etc. However the growth and properties of one dimensional ternary oxides such as $In_{2x}Al_{2-2x}O_3$ or $In_{2x}Ga_{2-2x}O_3$ have not been investigated widely. Ternary and quaternary oxides like $In_{2x}Ga_{2-2x}O_3$ [6] and $InGaO_3(ZnO)_5$ (IGZO) [7] have been used as transistors and the backplane of flat panel displays. More specifically $In_{2x}Ga_{2-2x}O_3$ is attractive because it has a very low optical absorption coefficient on the order of a few hundreds cm^{-1} in the visible range, a refractive index of around 1.65 and an energy band-gap of about 3.4 eV. On the other hand the main advantage of IGZO is that it can be deposited in the amorphous phase while retaining a high carrier mobility. One of the main issues concerning the fabrication of nanoscale devices using MO NWs is controlling the surface properties which are necessary to prevent fluctuations in their conductivity due to the adsorption and desorption of oxygen or water. This has been carried out on ZnO and SnO_2 NWs using polyimide and poly methyl methacrylate respectively [8,9]. Sulfur passivation has been used to improve mainly the properties of III-V NWs, but recently we investigated the effect of sulfur on the structural, electrical and optical properties of SnO_2 NWs and their conversion into SnS_2 NWs [10], while we have also shown that post growth processing of Sn doped In_2O_3 NWs under H_2S between 100°C to 600°C resulted into the appearance of band edge photoluminescence (PL) at 3.5 eV close to the energy band gap of In_2O_3, but no emission in the red or near Infra-Red (IR) [11]. More importantly Cu_2SnS_3/SnO_2 and $CuInS_2/Sn:In_2O_3$ NWs with ultraviolet PL at 3.7 eV were obtained *via* the deposition of 60 nm Cu over SnO_2 and Sn doped In_2O_3 NWs and processing under H_2S at 500°C [12]. Consequently the sulfur doping of MO NWs may be used to obtain metal oxy-sulfides (MOxS) NWs with different electrical and optical properties similar to β-$In_2S_{3-3x}O_{3x}$ [13] which has an optical band gap found to vary from 2.1 eV in pure β-In_2S_3 to 2.9 eV when it contained 8.5 at.% of oxygen and has been proposed as an alternative to CdS buffer layers in $Cu(In_xGa_{1-x})Se_2$ (CIGS) solar cells. CIGS is a direct band gap semiconductor, with a high light absorption coefficient, and CIGS solar cells exhibit high efficiencies greater than 20%. Hence CIGS/Cu_2S core-shell nanowire solar cells (NWSCs) have also been fabricated [14] while Peng *et al.* [15] prepared $CuInSe_2$ NWs using the vapor–liquid–solid (VLS) mechanism. Similarly $Cu(In_xGa_{1-x})S_2$ is a chalcopyrite material with a near-optimum band gap of 1.5 eV and contains S as opposed to Se which is toxic. However only few efforts have been devoted to the synthesis, properties and application of I–III–VI$_2$ chalcopyrite $Cu(In_xGa_{1-x})S_2$ NWs in solar cells [16].

Considering the above we have carried out a systematic investigation into the growth of $In_{2x}Ga_{2-2x}O_3$ NWs *via* the VLS mechanism by varying the In to Ga ratio but also the effect of S on its properties. The $In_{2x}Ga_{2-2x}O_3$ NWs have average diameters of ≈ 50 nm, lengths up to 100 μm and consist of a mixture of phases belonging to the binary constitutent components *i.e.* the cubic bixbyite crystal structure of In_2O_3 and monoclinic β-Ga_2O_3. The $In_{2x}Ga_{2-2x}O_3$ NWs exhibited PL at 400 nm or 3.1 eV which shifted to 1.8 eV after post growth processing under H_2S well above 500°C due to deep, donor to acceptor transitions and the formation of Ga rich $In_{2x}Ga_{2-2x}S_3$. In contrast, we find that the deposition of Cu over the $In_{2x}Ga_{2-2x}O_3$ NWs and post growth processing

Correspondence to: Matthew Zervos, Nanostructured Materials and Devices Laboratory, Department of Mechanical and Manufacturing Engineering,University of Cyprus, 20537, Nicosia, 1678, Cyprus, Tel: +357 22892194; Fax: +357 22892254; **E-mail:** zervos@ucy.ac.cy

Received: September 15, 2015; **Accepted:** November 05, 2015; **Published:** November 10, 2015

under H_2S at lower temperatures between 100°C to 500°C resulted into $Cu(In_xGa_{1-x})S_2$ NWs with smaller resistances compared to the as-grown or S doped $In_{2x}Ga_{2-2x}O_3$ NWs and a stronger red shift of the PL that changed from 3.1 eV to 1.5 eV close to the energy band gap of of I–III–VI_2 chalcopyrite $Cu(In_xGa_{1-x})S_2$.

Methods

$In_{2x}Ga_{2-2x}O_3$ NWs were grown using a low-pressure chemical vapour deposition (LPCVD) reactor consisting of a 1″ quartz tube, capable of reaching 1100°C, that was fed from a manifold consisting of four mass flow controllers fed with Ar, O_2, NH_3 and H_2. For the growth of the $In_{2x}Ga_{2-2x}O_3$ NWs, Sn (Aldrich, 2-14 Mesh, 99.9%), In and Ga (Aldrich, 99.9%) were weighed with an accuracy of ± 1 mg. Square samples of Si(001) ≈ 7 mm x 7 mm were cleaned sequentially in trichloroethylene, methanol, acetone, isopropanol, rinsed with de-ionised water , dried with nitrogen and coated with ≈ 1 nm Au by sputtering. Following this 0.2 g of In and Ga containing a trace of 1 % Sn and the 1 nm Au/Si(001) substrates were loaded inside a quartz boat which was positioned at the centre of the 1″ tube that was pumped down to 10^{-4} mBar and subsequently purged with 600 sccms of Ar for 10 min at 1 mBar after which the temperature was ramped up to 800°C using a ramp rate of 30°C/min while maintaining the same flow of Ar. Upon reaching 800°C, a small flow of 10 sccms O_2 was added to the main flow of Ar in order to grow the $In_{2x}Ga_{2-2x}O_3$ NWs after which the reactor was allowed to cool down without O_2. The morphology of the $In_{2x}Ga_{2-2x}O_3$ NWs was determined by scanning electron microscopy (SEM) while their crystal structure was determined by x-ray diffraction (XRD) using a Rigaku Miniflex. Subsequently the $In_{2x}Ga_{2-2x}O_3$ NWs were exposed to 50 sccm H_2S between 100°C to 700°C for 60 min using a ramp rate of 10°C/min in a different reactor capable of reaching 1500°C. All of the $In_{2x}Ga_{2-2x}O_3$ NWs were inspected by SEM after exposure to H_2S in order to determine changes in morphology, while their crystal structure and phase purity was determined again by XRD. The photoluminescence (PL) spectra of the as grown and S doped $In_{2x}Ga_{2-2x}O_3$ NWs on Si(001) were obtained at room temperature using an excitation of 266 nm. Finally we deposited 40 nm of Cu over the $In_{2x}Ga_{2-2x}O_3$ NWs and processed these under H_2S between 100°C to 500°C after which their properties were determined in the same way as described above. The resistance of the $In_{2x}Ga_{2-2x}O_3$ NW networks that were grown on 10 mm x 10 mm quartz and $Cu(In_xGa_{1-x})S_2$ NW obtained after the deposition of Cu and processing under H_2S was measured in accordance with O'Dwyer using In contacts [17].

Results and discussion

We will begin with a discussion of the binary oxides, namely In_2O_3 and Ga_2O_3, which is necessary to understand the growth and properties of the $In_{2x}Ga_{2-2x}O_3$ NWs. We have shown previously that In_2O_3 NWs with lengths up to ≈ 1 µm and average diameters of ≈ 50 nm can be obtained on 1 nm Au/Si(001) at 700°C and 1 Atm *via* the reaction of In and O_2 [3] but the yield and uniformity was limited up to ≈ 10 mm from the metal sources. In contrast, a significantly higher yield and uniform distribution of Sn doped In_2O_3 with lengths up to ≈ 100 µm and diameters of ≈ 50 nm were obtained by LPCVD at 800°C on 1 nm Au/Si(001) over distances greater than 10 mm [4]. This is a direct consequence of the larger metal vapor pressure of Sn and In at 10^{-1} mBar and 800°C. The Sn doped In_2O_3 NWs grow *via* the VLS mechanism, have a cubic bixbyite crystal structure, metallic like conductivities and exhibited PL at 2.4 eV while post growth processing under H_2S up to 400°C resulted into the emergence of PL at 3.5 eV due to band edge emission from In_2O_3 but no PL in the red or near infra red (IR) [11]. Similar to the case of In_2O_3 the reaction of Ga with O_2 at 900°C and 1 Atm lead to the growth of β-Ga_2O_3 NWs on 1 nm Au/Si(001) but the yield and uniformity was not satisfactory. The β-Ga_2O_3 NWs had a monoclinic β-Ga_2O_3 crystal structure and exhibited PL with a maximum at 520 nm or 2.4 eV attributed to oxygen vacancies and states lying energetically in the upper half of the energy band gap of β-Ga_2O_3 as shown by ultrafast absorption-transmission spectroscopy [18]. A higher yield and uniform distribution of Sn doped Ga_2O_3 NWs was obtained by LPCVD at 800°C and 1 mBar. The Sn doped Ga_2O_3 NWs had a monoclinic crystal structure and exhibited PL at 3.5 eV while post growth processing under H_2S above 500°C resulted into the emergence of PL at 1.8 eV. This red emission from the β-Ga_2S_3 NWs was attributed to deep donor to acceptor transitions and was exploited for improving the efficiency of a Si solar cell *via* spectral shifting [19].

Here we have grown Sn doped $In_{2x}Ga_{2-2x}O_3$ NWs by LPCVD at 800°C and 1 mBar using Sn , In and Ga metal sources containing 13, 30, 35, 40, 50, 70, 75 % Ga and only 1% Sn. The vapor pressures of In and Ga at 800°C are ≈ 10^{-4} and 10^{-5} mBar respectively while In and Ga have similar ionic radii which renders feasible the compositional tuning of $In_{2x}Ga_{2-2x}O_3$ NWs. We obtained a high yield and good uniformity of $In_{2x}Ga_{2-2x}O_3$ NWs with average diameters of ≈ 50 nm and lengths up to 100 µm. A typical SEM image is shown in Figure 1a. We find that the $In_{2x}Ga_{2-2x}O_3$ NWs do not grow on plain Si so one dimensional growth occurs *via* the VLS mechanism, as depicted schematically in Figure1b, similar to Sn doped In_2O_3 where it has been shown that the Au nanoparticles at the top of the Sn doped In_2O_3 NWs are in fact rich in Sn not In [20]. The $In_{2x}Ga_{2-2x}O_3$ NWs exhibited clear peaks in the XRD as shown in Figure 2 from which they appear to consist of a mixture of phases belonging to the binary constituent components *i.e.* the cubic bixbyite crystal structure of In_2O_3 and monoclinic β-Ga_2O_3. There are few reports on the synthesis of pure $In_{2x}Ga_{2-2x}O_3$ and the highest conductivities have been obtained using Sn as a dopant [21]. Solid solutions of $In_{2x}Ga_{2-2x}O_3$, where $x < 0.4$, has been shown to result in indium substitution into the β-Ga_2O_3 lattice, while $x > 0.95$, results in gallium substitution into the cubic In_2O_3 lattice. For $0.4 < x < 0.95$ phase segregation occurs and results in β-Ga_2O_3 and an In_2O_3-Ga_2O_3 phase with the cubic In_2O_3 structure [22]. It is worthwhile pointing out that the structural, electronic, and optical properties of $In_{2x}Ga_{2-2x}O_3$ have been determined recently by hybrid density functional methods and it has been shown that the structure of $In_{2x}Ga_{2-2x}O_3$ is similar to β-Ga_2O_3 but it is distinct from Ga doped In_2O_3 [23]. We find that the XRD spectra of the $In_{2x}Ga_{2-2x}O_3$ NWs obtained using 25 to 70% Ga contain a few weak, but nevertheless well resolved peaks, that do not belong to In_2O_3 or β-Ga_2O_3 as shown in Figure 2 but must belong to a Ga rich $In_{2x}Ga_{2-2x}O_3$ phase since they do not correspond to SnO_2. Before elaborating further, it is worthwhile pointing out that we tried to grow $In_{2x}Al_{2-2x}O_3$ NWs *via* the VLS mechanism but we found from high resolution XRD that the Al was not incorporated in the crystal lattice of In_2O_3 due to the large difference in the ionic radii of Al and In but also due to the fact that Al has a very large affinity to oxygen which is known prevent one dimensional growth *via* the VLS mechanism [24]. Besides we did not observe a mixture of In_2O_3 and Al_2O_3 phases in the XRD and did not detect more than 1% Al by energy dispersive x-ray analysis (EDX) which is different to the case of the $In_{2x}Ga_{2-2x}O_3$ NWs. A typical EDX spectrum obtained from the $In_{2x}Ga_{2-2x}O_3$ NWs obtained with 25% Ga is shown in Figure 1b from which we observe distinct peaks belonging to In and Ga. This clearly shows that the In and Ga are incorporated in the $In_{2x}Ga_{2-2x}O_3$ NWs while the % at. content of In and Ga in the $In_{2x}Ga_{2-2x}O_3$ NWs obtained using metal sources containing different ratios of In to Ga is shown as an inset in Figure 1(c). It is

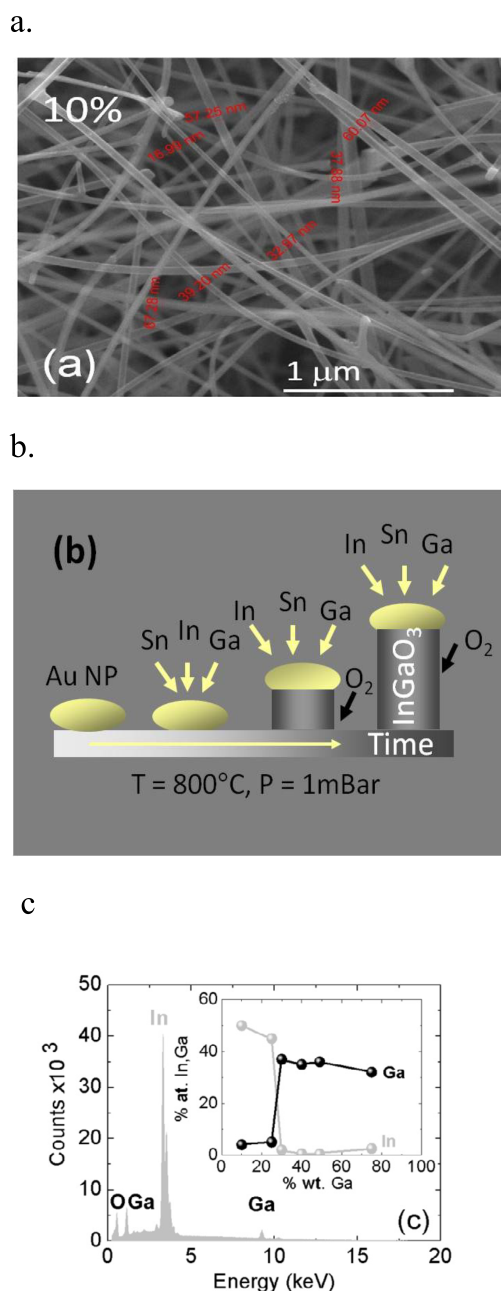

Figure 1: (a) SEM image of the $In_{2x}Ga_{2-2x}O_3$ NWs obtained with 10 wt. % Ga (b) corresponding EDX spectrum of $In_{2x}Ga_{2-2x}O_3$ with 25% Ga ; inset shows variation of the % at. In and Ga in the $In_{2x}Ga_{2-2x}O_3$ NWs versus the ratio of Ga to In metal sources (c) schematic diagram of the VLS growth mechanism for one dimensional growth of the $In_{2x}Ga_{2-2x}O_3$ NWs.

evident that one may tune the actual composition of the $In_{2x}Ga_{2-2x}O_3$ NWs over a broad range in contrast to the case of $In_{2x}Al_{2-2x}O_3$ NWs. These findings are similar to the case of Sn doped In_2O_3 NWs where we showed that it is possible to tune the crystal structure from cubic bixbyite In_2O_3 to tetragonal rutile SnO_2 *via* a regime consisting of a mixture of In_2O_3 and SnO_2 [4]. Recently we showed that the same is also true for Sn doped Ga_2O_3 NWs. Both Sn doped In_2O_3 and Sn doped Ga_2O_3 NWs were grown by LPCVD at 800°C and 1mBar which are exactly the same growth conditions used for the growth of the Sn doped $In_{2x}Ga_{2-2x}O_3$ NWs. The ability to tune the composition of the $In_{2x}Ga_{2-2x}O_3$ NWs is attributed to the fact that its constituent binary oxide components can be grown using exactly the same growth conditions and Sn as a dopant but also due to the similar ionic radii of In and Ga. A schematic illustration of the VLS growth mechanism is shown for completeness in Figure 1b. All of the $In_{2x}Ga_{2-2x}O_3$ NWs showed PL with a maximum between 350 nm to 400 nm as shown in Figure 3a and a tail extending to 500 nm which is attributed to the existence of oxygen vacancies and states lying energetically in the upper half of the energy band gap of the $In_{2x}Ga_{2-2x}O_3$ NWs, as shown previously using ultrafast absorption transmission spectroscopy in the case of the β-Ga_2O_3 or In_2O_3 MO NWs. Interestingly we find that the PL of the $In_{2x}Ga_{2-2x}O_3$ NWs grown using more than 30 % Ga is slightly blue shifted, which is consistent with a change in the composition of the $In_{2x}Ga_{2-2x}O_3$ NWs from In to Ga rich and results into an increase in energy band gap. More specifically the PL has a maximum at 400 nm or 3.1 eV for 10 to 30% Ga but shifts to 350 nm or 3.5 eV above 30% Ga which is close to the experimental energy band gaps of bulk $In_{2x}Ga_{2-2x}O_3$.

The $In_{2x}Ga_{2-2x}O_3$ NWs were further processed under H_2S at 500°C, 700°C and 900°C in order to determine their optical properties before the deposition of Cu and their conversion to $Cu(In_xGa_{1-x})S_3$ NWs. It is known that H_2S undergoes complete decomposition on the surface of oxides, even at room temperature, and the S atoms bond to the metal cations of the surface. The ionic radii of O^{2-} and S^{2-} are 1.32 Å and 1.82 Å respectively meaning that S will also diffuse into the $In_{2-x}Ga_xO_3$ and hence S^{2-} will substitute O^{2-} or fill in vacancies. We find that the $In_{2-x}Ga_xO_3$ NWs processed under H_2S at 500°C showed PL at 3.5 eV but a red shift occurred to 1.8 eV following processing at 700°C and 900°C as shown in Figure 3b which is similar to the case of Sn

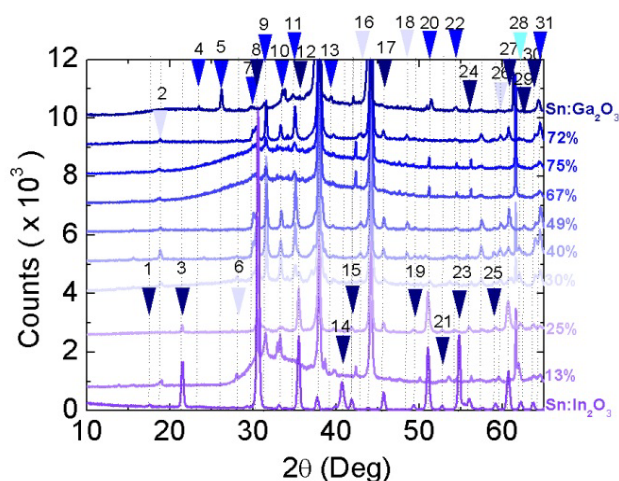

Figure 2. XRD of $In_{2x}Ga_{2-2x}O_3$ NWs grown using 13, 25, 30, 40, 49, 67, 72 and 75% Ga. Also shown for comparison of Sn doped In_2O_3 (bottom trace) and Sn doped Ga_2O_3 (top trace). The peaks have been labeled for clarity with arrows in ascending order and increasing angle as follows :

1► 17.54°(010)In_2O_3, 2► 18.84°$In_{2x}Ga_{2-2x}O_3$, 3► 21.44°(022)In_2O_3, 4► 23.44°(012)Ga_2O_3, 5► 26.20°(-012)Ga_2O_3, 6► 28.06°$In_{2x}Ga_{2-2x}O_3$, 7► 29.78°(400)Ga_2O_3, 8► 30.56°(200) In_2O_3, 9► 31.30°(002)Ga_2O_3, 10► 33.06°(101)Ga_2O_3, 11► 35.04°(111)Ga_2O_3, 12► 35.46°(400)In_2O_3, 13► 39.42°(-112)Ga_2O_3, 14► 40.66°(332)In_2O_3, 15► 41.82°(422) In_2O_3, 16► 42.98°$In_{2x}Ga_{2-2x}O_3$, 17► 45.68°(134)In_2O_3, 18► 48.50°$In_{2x}Ga_{2-2x}O_3$, 19► 49.26°(600)In_2O_3, 20► 51.42°(12)Ga_2O_3, 21► 52.80°(433)In_2O_3, 22► 54.32°(-113)Ga_2O_3, 23► 54.74°(611)In_2O_3, 24► 56.20°(026)In_2O_3, 25► 59.12°(622) In_2O_3, 26► 59.74° $In_{2x}Ga_{2-2x}O_3$, 27► 60.07°(136) In_2O_3, 28► 62.04°(301) SnO_2, 29► 62.58°In_2O_3 (444) 30► 63.58°(543)In_2O_3, 31► 64.34°(121)Ga_2O_3.

The peaks belonging to Sn doped In_2O_3 are labeled with dark blue ► arrows and those of Sn doped Ga_2O_3 with ► blue. A few weak but well resolved peaks appear to belong to a Ga rich $In_{2x}Ga_{2-2x}O_3$ are labelled with lighter color. Only one peak has been identified as belonging to SnO_2.

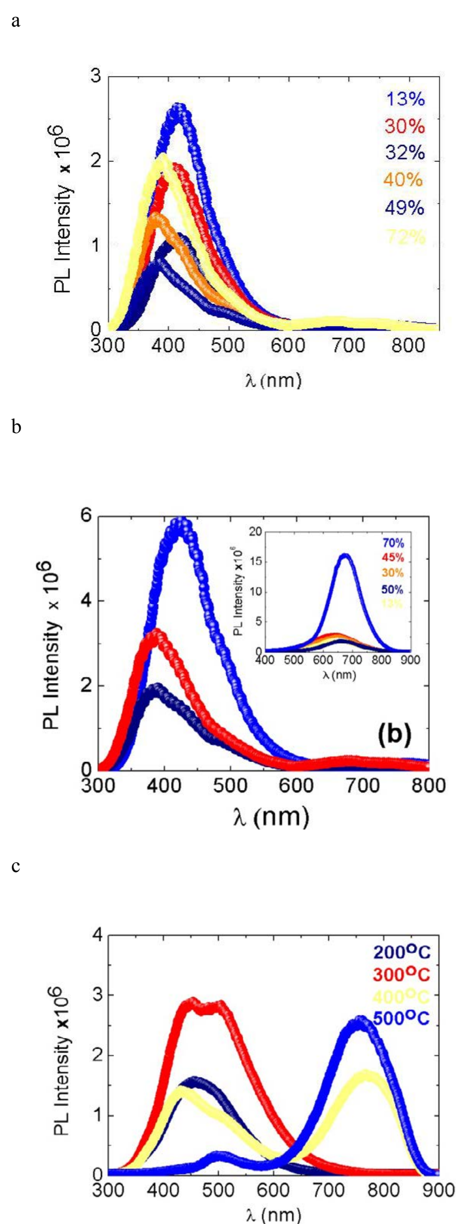

Figure 3: (a) Room temperature PL of as-grown $In_{2x}Ga_{2-2x}O_{3}$ NW obtained using different % Ga content metal source **(b)** Room temperature PL of $In_{2x}Ga_{2-2x}O_{3}$ NWs after processing under $H_{2}S$ at 500°C; inset shows the PL after processing under $H_{2}S$ at 700°C **(c)** PL of chalcopyrite $Cu(In_{x}Ga_{1-x})S_{3}$ NWs obtained by deposition of 40 nm Cu over the $In_{2x}Ga_{2-2x}O_{3}$ NWs grown using 30% Ga and processing under $H_{2}S$ at 200°C, 300°C, 400°C and 500°C.

doped $Ga_{2}O_{3}$ NWs. This red emission is attributed to deep donor to acceptor state recombination similar to what has been observed by in the case of two dimensional $Ga_{2}S_{3}$ [25]. One may observe in fact, that the PL intensity of the S doped $In_{2-x}Ga_{x}O_{3}$ NWs, becomes stronger with increasing Ga content, suggesting that the red emission is related to the formation of β-$Ga_{2}S_{3}$ [19]. All of the S doped $In_{2-x}Ga_{x}O_{3}$ NWs had very high resistances, in excess of 100 MΩ consistent with the high resistances measured in the case of $Ga_{2}S_{3}$ [25]. However we find that the deposition of 40 nm Cu over $In_{2-x}Ga_{x}O_{3}$ NWs and post growth processing under $H_{2}S$ at 100°C, 200°C, 300°C, 400°C and 500°C resulted into $Cu(In_{x}Ga_{1-x})S_{2}$ NW networks with smaller resistances of the order of 100 kΩ. More interestingly we find that the PL shifts from 3.1 eV to 1.55 eV after processing at 500°C, as shown in Figure 3c, which is different to the case of the plain $In_{2-x}Ga_{x}O_{3}$ NWs that exhibit PL at 3.1 eV after processing under $H_{2}S$ at 500°C. Note also that the PL of the $In_{2-x}Ga_{x}O_{3}$ NWs has a maximum at 1.8 eV after processing at 700°C so the emission at 1.55 eV is most likely related to the formation of chalcopyrite $Cu(In_{x}Ga_{1-x})S_{2}$ which has an energy band gap of 1.5 eV. We found that the $Cu(In_{x}Ga_{1-x})S_{2}$ NWs obtained from $In_{2-x}Ga_{x}O_{3}$ NWs with 30% Ga have a completely different XRD pattern compared to the S doped $In_{2-x}Ga_{x}O_{3}$ NWs, both of which were processed at 500°C. This is similar to the formation of $CuInS_{2}$ which we observed recently following the deposition of Cu over Sn doped $In_{2}O_{3}$ NWs and post growth processing under $H_{2}S$ at 500°C [12]. In effect the Cu and S will diffuse and react with the $In_{2-x}Ga_{x}O_{3}$ NWs at elevated temperatures. Lower temperatures do not favor the diffusion of Cu and S so the PL has a maximum at 450 nm to 500 nm but the resistance of the resultant $Cu_{2}S/In_{2-x}Ga_{x}O_{3}$ core-shell NW networks was of the order of a few Ω.

Conclusion

We have grown $In_{2x}Ga_{2-2x}O_{3}$ NWs at 800°C *via* the VLS mechansism on Si(001) using Au as a catalyst and varied systematically the In to Ga ratio. The $In_{2x}Ga_{2-2x}O_{3}$ NWs have average diameters of ≈ 50 nm, lengths up to 100 μm and consist of a mixture of distinct phases belonging to cubic bixbyite $In_{2}O_{3}$ and monoclinic $Ga_{2}O_{3}$. All $In_{2x}Ga_{2-2x}O_{3}$ NWs exhibited room temperature PL at 400 nm or 3.1 eV which shifted slightly to the blue upon increasing the content of Ga. In contrast we observed a strong red-shift in the PL from 3.1 to 1.8 eV after post growth processing under $H_{2}S$ above 500°C which is attributed to the formation of Ga rich $In_{2x}Ga_{2-2x}S_{3}$. More importantly the deposition of Cu over the $In_{2x}Ga_{2-2x}O_{3}$ NWs and post growth processing under $H_{2}S$ at lower temperatures between 100°C to 500°C resulted into I–III–VI_{2} chalcopyrite $Cu(In_{x}Ga_{1-x})S_{3}$ NWs with smaller resistances compared to the as-grown and S doped $In_{2x}Ga_{2-2x}O_{3}$ NWs but also a stronger red shift of the PL from 3.1 to 1.5 eV which is close to the energy band gap of $Cu(In_{x}Ga_{1-x})S_{3}$.

References

1. Law M, Greene LE, Johnson JC, Saykally R, Yang P (2005) Nanowire dye-sensitized solar cells. Nanowire dye-sensitized solar cells.*Nat Mater* 4: 455-459. [Crossref]

2. Tsokkou D, Othonos A, Zervos M (2012) Carrier dynamics and conductivity of SnO2 nanowires investigated by time-resolved terahertz spectroscopy.*ApplPhysLett* 100: 133101.

3. Tsokou D, Zervos M, Othonos A (2009) Ultrafast time-resolved spectroscopy of In2O3 nanowires. *J ApplPhys*106: 084307.

4. Zervos M, Mihailescu, Giapintzakis J, Othonos A (2014) Broad compositional tunability of indium tin oxide nanowires grown by the vapor-liquid-solid mechanism. *ApplPhysLettMat* 2: 056104.

5. Lopez I, Castaldini A, Cavallini A, Nogales E (2014) *J Phys D ApplPhys* 47: 415104.

6. Presley R, Hong D, Chiang H, Hung C, Hoffman R, et al (2006) Transparent ring oscillator based on indium gallium oxide thin-film transistors.*Sol Stat Elect* 50: 500.

7. Nomura K, Ohta H, Ueda K, Kamiya T, Hirano M, et al. (2003) Thin-film transistor fabricated in single-crystalline transparent oxide semiconductor. *Science* 300: 1269-1272.[Crossref]

8. Huh J, Joo MK, Jang D, Lee JH, Kim GT, (2012) Reduced charge fluctuations in individual SnO 2 nanowires by suppressed surface reactions. *J Mater Chem*22: 24012.

9. Park WI, Kim JS, Yi GC, Bae MH, Lee HJ (2004) Fabrication and electrical characteristics of high-performance ZnOnanorod field-effect transistors. *ApplPhysLett*85: 5052.

10. Zervos M, Mihailescu CN, Giapintzakis J, Othonos A, Luculescu CR (2015) Surface

passivation and conversion of SnO 2 to SnS 2 nanowires. *Materials Science and Engineering* 198: 10-13.[Crossref]

11. Zervos M, Mihailescu CN, Giapintzakis J, Othonos A, Travlos A, et al. (2015) Electrical, structural, and optical properties of sulfurized Sn-doped In2O 3 nanowires. *Nanoscale Res Lett*10: 995.[Crossref]
12. Karageorgou E,Zervos M, Othonos A (2014) Sulfur doping of M/In2O3 (M= Al, W) nanowires with room temperature near infra red. *PhysLettMat* 2: 116107.
13. Barreau N,Marsillac S,Albertini D,Bernede J (2002) Structural, optical and electrical properties of β-In 2 S 3-3x O 3x thin films obtained by PVD.*Thin Solid Films* 403: 331.
14. Inguanta R,Livreri P,Piazza S,Sunseri C (2010) *Electrochem Sol Stat Lett*13: 22.
15. Peng H, Schoen DT, Meister S, Zhang XF, Cui Y (2007) Synthesis and phase transformation of In(2)Se(3) and CuInSe(2) nanowires. *J Am ChemSoc*129: 34-35.[Crossref]
16. Chen LZ,LiaoJD,Chuang YJ (2011) Synthesis and characterization of chalcopyrite quaternary semiconductor Cu (In x Ga 1− x) S 2 nanowires by electrospun route.*Thin Solid Films*519: 3658.
17. O'Dwyer C, Szachowicz M, Visimberga G, Lavayen V, Newcomb SB, et al. (2009) Bottom-up growth of fully transparent contact layers of indium tin oxide nanowires for light-emitting devices. *Nat Nanotechnol*4: 239-244.[Crossref]
18. Othonos A,Zervos M,Christofides C (2010) Carrier dynamics in β-Ga2O3 nanowires. *Journal of Applied Physics*108: 124302.
19. Othonos KM, Zervos M, Christofides C, Othonos A (2015) Ultrafast Spectroscopy and Red Emission from Î²-Ga2O 3/Î²-Ga 2S 3 Nanowires. *Nanoscale Res Lett*10: 1016.[Crossref]
20. Gao J,Chen R,Li DH,Jiang L,Ye J, et al.(2011) UV light emitting transparent conducting tin-doped indium oxide (ITO) nanowires.*Nanotechnology*22: 195706.
21. Phillips JM,Kwo J,Thomas GA,Carter SA (1994)Transparent conducting thin films of GaInO3.*ApplPhysLett* 65: 115.
22. Edwards DD,Folkins P,Mason T (1997) Phase Equilibria in the Ga2O3In2O3 System. *J AmerCerSoc*80: 253.
23. Wang V,Xiao W,Ma DM, Liu RJ, Yang CM (2014) Structural, electronic, and optical properties of GaInO3: A hybrid density functional study. *J ApplPhys*115: 043708
24. Zervos M,Mihailescu C,Giapintzakis J,Othonos A (2015) Sulfur doping of M/In2O3 (M= Al, W) nanowires with room temperature near infra red emission. *AIPAdvances* 5: 097101.
25. Ho CH, Chen HH (2014) optically decomposed near-band-edge structure and excitonic transitions in Ga2S3.*Scientific Reports* 4: 6143.

Copyright: ©2015 Zervos M. This is an open-access article distributed under the terms of the Creative Commons Attribution License, which permits unrestricted use, distribution, and reproduction in any medium, provided the original author and source are credited.